

# VISEM-Tracking: Human Spermatozoa Tracking Dataset

Vajira Thambawita<sup>1,†</sup>, Steven A. Hicks<sup>1,†</sup>, Andrea M. Storås<sup>1,2,†</sup>, Thu Nguyen<sup>1</sup>, Jorunn M. Andersen<sup>2</sup>, Oliwia Witczak<sup>2</sup>, Trine B. Haugen<sup>2</sup>, Hugo L. Hammer<sup>2,1,†</sup>, Pål Halvorsen<sup>1,2</sup>, and Michael A. Riegler<sup>1,3,†</sup>

<sup>1</sup>SimulaMet, Oslo, Norway

<sup>2</sup>OsloMet, Oslo, Norway

<sup>3</sup>University of Tromsø, Norway

\*corresponding author(s): Vajira Thambawita (vajira@simula.no)

†these authors contributed equally to this work

## ABSTRACT

A manual assessment of sperm motility requires microscopy observation, which is challenging due to the fast-moving spermatozoa in the field of view. To obtain correct results, manual evaluation requires extensive training. Therefore, computer-assisted sperm analysis (CASA) has become increasingly used in clinics. Despite this, more data is needed to train supervised machine learning approaches in order to improve accuracy and reliability in the assessment of sperm motility and kinematics. In this regard, we provide a dataset called VISEM-Tracking with 20 video recordings of 30 seconds of wet sperm preparations with manually annotated bounding-box coordinates and a set of sperm characteristics analyzed by experts in the domain. In addition to the annotated data, we provide unlabeled video clips for easy-to-use access and analysis of the data via methods such as self- or unsupervised learning. As part of this paper, we present baseline sperm detection performances using the YOLOv5 deep learning model trained on the VISEM-Tracking dataset. As a result, we show that the dataset can be used to train complex deep learning models to analyze spermatozoa. The dataset is publicly available at <https://zenodo.org/record/7293726>.

## Background & Summary

Machine learning (ML) is increasingly being used to analyze videos of spermatozoa under a microscope for developing computer-assisted sperm analysis (CASA) systems<sup>1,2</sup>. In the last few years, several studies have investigated the use of deep neural networks (DNNs) to automatically determine specific attributes of a semen sample, like predicting the proportion of progressive, non-progressive, and immotile spermatozoa<sup>3-7</sup>. However, a major challenge with using ML for semen analysis is the general lack of data for training and validation. Only a few open labeled datasets exist (Table 1), with most focus on still-frames of fixed and stained spermatozoa, or very short sequences of sperm to analyze the morphology of the spermatozoa.

In this paper, we present a multi-modal dataset containing videos of spermatozoa with the corresponding manually annotated bounding boxes (localization) and additional clinical information about the sperm providers from the original study<sup>15</sup>. This dataset is an extension of our previously published dataset VISEM<sup>15</sup>, which included videos of spermatozoa labeled with quality metrics following the World Health Organization (WHO) recommendations<sup>16</sup>. There have been several datasets related to spermatozoa as follows.

For example, Ghasemian et al.<sup>8</sup> have published an open sperm dataset called HSMA-DS: Human Sperm Morphology Analysis DataSet with normal and abnormal sperm cells. Experts annotated different features, namely vacuole, tail, midpiece, and head abnormality. The availability of abnormalities of these features were marked using binary notations such as 1 or 0, 1 is for abnormal, and 0 for normal. In total, there are 1,457 sperm cells for morphology analysis. These sperm cell images were captured with  $\times 400$  and  $\times 600$  magnification. The Modified Human Sperm Morphology Analysis Dataset (MHSMA)<sup>9</sup> consists of 1,540 cropped images from the HSMA-DS dataset<sup>8</sup>. This dataset was collected for analyzing different parts of sperm cells (morphology). The maximum image size in the dataset is  $128 \times 128$  pixels.

The HuSHEM<sup>10</sup> and SCIAN-MorphoSpermGS<sup>11</sup> datasets consist of images of sperm heads captured from fixed and stained semen smears. The main purpose of these datasets is sperm morphology classification into five categories, namely normal, tapered, pyriform, small, and amorphous. SMIDS<sup>12</sup> is another dataset consisting of 3000 images cropped from 200 stained ocular images from 17 subjects between 19 – 39 years. From 3000 images, 2027 patches were manually annotated as normal and abnormal. Other 973 samples were classified as non-sperm using spatial-based automated features. McCallum et al.<sup>13</sup> have published another similar dataset with bright-field sperm cells of six healthy participants within 1064 cropped images. The main purpose of this dataset is to find correlations between sperm cells and DNA quality. However, these datasets do not

**Table 1.** Overview of existing sperm datasets.

Author	Name/Title	Ground Truth	# Images	# Videos	Summary
Ghasemian et al. <sup>8</sup>	HSMA-DS: Human Sperm Morphology Analysis DataSet	Classification	1457	-	This dataset is for morphology analysis and the dataset consists of captured sperm cells with $\times 400$ and $\times 600$ magnification
Javadi et al. <sup>9</sup>	MHSMA: Modified Human Sperm Morphology Analysis Dataset	Classification	1,540	-	The dataset is for morphology analysis. This dataset consists of only sperm heads cropped from different samples collected from 235 participants
Shaker et al. <sup>10</sup>	HuSHeM: Human Sperm Head Morphology	Classification	216	-	HuSHeM is for sperm morphology classification. Semen smears were fixed and stained. Contain sperm head images of $131 \times 131$ pixels. Four classes: normal, tapered, pyriform, and amorphous.
Violeta et al. <sup>11</sup>	SCIAN-MorphoSpermGS	Classification	1854	-	This dataset is for sperm morphology analysis. The data was classified into five classes: normal, tapered, pyriform, small, and amorphous.
Ilhan et al. <sup>12</sup>	SMIDS: Sperm Morphology Image Data Set	Classification	3000	-	For morphology analysis. The data was collected from 17 subjects. The dataset has manually annotated two classes: normal and abnormal and an automatically extracted class: Non-sperm.
McCallum et al. <sup>13</sup>	-	Classification	1,064	-	Bright-field sperm cell images are $150 \times 150$ pixels and cropped from images of six healthy donors.
Chen et al. <sup>14</sup>	SVIA: Sperm Videos and Images Analysis dataset	Detection, segmentation and classification	4041	101 (1-2 seconds)	The dataset consists of 278,000 annotated objects under three subsets. The data can be used for object detection (125,000 annotations), segmentation (26,000 annotations), and classification (125,880 cropped objects from the images).
Haugen et al. <sup>15</sup>	VISEM	Regression	-	85	The dataset consists of 85 videos of $640 \times 480$ at 50 FPS. The ground truth files have manually assessed semen analysis data, fatty acids, sex hormones, and participant-related data.
<b>Ours</b>	<b>VISEM-Tracking</b>	<b>Detection, tracking, and regression</b>	29,196	20 (30 seconds)	<b>Our dataset contain 656,334 annotated objects with tracking details. More details about our dataset is discussed below.</b>

provide spermatozoa's motility and kinetics features.

Chen et al.<sup>14</sup> introduced a sperm dataset called SVIA (Sperm Videos and Images Analysis dataset), which contains 101 short 1 to 3 seconds video clips and corresponding manually annotated objects. The dataset is divided into three subsets, namely subset-A, B, and C. Subset-A contains 101 video clips (30 FPS) containing 125,000 object locations and corresponding

categories. Subset-B contains 10 videos with 451 ground truth segmentation masks and subset-C consists of cropped sperms for classification into 2 categories (impurity images and sperm images). The provided video clips are very short compared to VISEM-Tracking. Our dataset contains  $7\times$  more annotated video frames. In addition, VISEM-Tracking contains  $2.3\times$  more annotated objects compared to SVIA.

None of the above datasets provide motility features for analyzing sperm motility. In contrast to these datasets, we provide tracking identifiers that allow identifying the same sperm within a video sequence. In this regard, the amount of information contained in our dataset is consequently larger and more detailed than currently available, which opens up several exciting research directions in computer science but also from the biological perspective. For example, sperm tracking, classifying spermatozoa based on motility and analyzing movement patterns. More information about the data is discussed in the following sections. To the best of our knowledge, this is the first open dataset of its kind.

## Methods

The videos for this dataset were originally obtained to study overweight and obesity in the context of male reproductive function<sup>17,18</sup>. In the study, male participants aged 18 years or older were recruited between 2008 and 2013 from the normal population. Further details on the recruitment can be found in<sup>15</sup>. The study was approved by the Regional Committee for Medical and Health Research Ethics, South East, Norway (REK number: 2008/3957), and all participants provided written informed consent. The original project was finished in December 2017, and all data was fully anonymized.

The samples to be recorded were placed on a heated microscope stage (37°C) and examined under a  $400\times$  magnification using an Olympus CX31 microscope. The videos were recorded by a microscope-mounted UEye UI-2210C camera made by IDS Imaging Development Systems in Germany. The videos are saved as AVI files. Motility assessment was performed based on the videos following the WHO recommendations<sup>16</sup>.

The bounding box annotation was performed by data scientists in close collaboration with researchers in the field of male reproduction. The data scientists labeled each video using the tool LabelBox<sup>1</sup>, which was then verified by the three biologists to ensure that the annotations were correct. Moreover, in addition to the per sperm tracking annotation, we also provide additional labels per spermatozoa, which are: 'normal sperm', 'pinhead', and 'cluster'. The pinhead category consists of spermatozoa with abnormally small black heads within the view of the microscope. The cluster category consists of several spermatozoa grouped together. Sample annotations are presented in Figure 1. The red boxes represent normal spermatozoa cells which constitute the majority of this dataset and are also biologically most relevant. The green boxes represent sperm clusters where few spermatozoa cells are clustered together, making it hard to annotate sperm cells separately. The blue color boxes represent small or pinhead spermatozoa which are smaller than normal spermatozoa and have very small heads compared to a normal sperm head.

## Data Records

The VISEM-Tracking dataset contains 20 videos, each with a fixed duration of 30 seconds with the corresponding annotated bounding boxes. The 20 were chosen based on how different they are to all the videos in the dataset in order to obtain as many diverse tracking samples as possible. Since each video from the original dataset lasts for more than 30 seconds we also provide, in addition to the annotated video clips, the remaining video as 166 30 seconds video clips for the 20 annotated videos and 336 30 seconds video clips for all unlabelled videos of the VISEM dataset<sup>15</sup> that were not used to provide tracking information. This was done to make it easy to use for future studies that aim to explore more advanced methods such as semi- or self-supervised learning<sup>19</sup>.

A length of 30 seconds was chosen to make it easier to annotate and process the video files. These videos can also be used for a possible extension of the tracking data in the future. The splitting process of the long videos is presented in Figure 2. More details about the dataset itself are summarized in Table 2.

The folder containing annotated videos has 20 sub-folders with annotations of each video. Each folder of videos has a folder containing extracted frames of the video, a folder containing bounding box labels of each frame, and a folder containing bounding box labels and the corresponding tracking identifiers. In addition to these, a complete video file (.mp4) is provided in the same folder. All bounding box coordinates are given using the YOLO<sup>20</sup> format. The folder containing bounding box details with tracking identifiers has '.txt' files with unique tracking ids to identify individual spermatozoa throughout the video. It is worth noting that the area of the bounding boxes of the same sperm is changing over time depending on its position and movement in the videos as depicted in Figure 3. Moreover, the text files contain class labels, 0: normal sperm, 1: sperm clusters, and 2: small or pinhead sperm.

In most of the labeled videos, each frame contains bounding box information (1,470 frames on average per video). The video titled *video\_23* has 174 frames without spermatozoa. Furthermore, some videos are recorded at different frame rates

---

<sup>1</sup><https://labelbox.com>

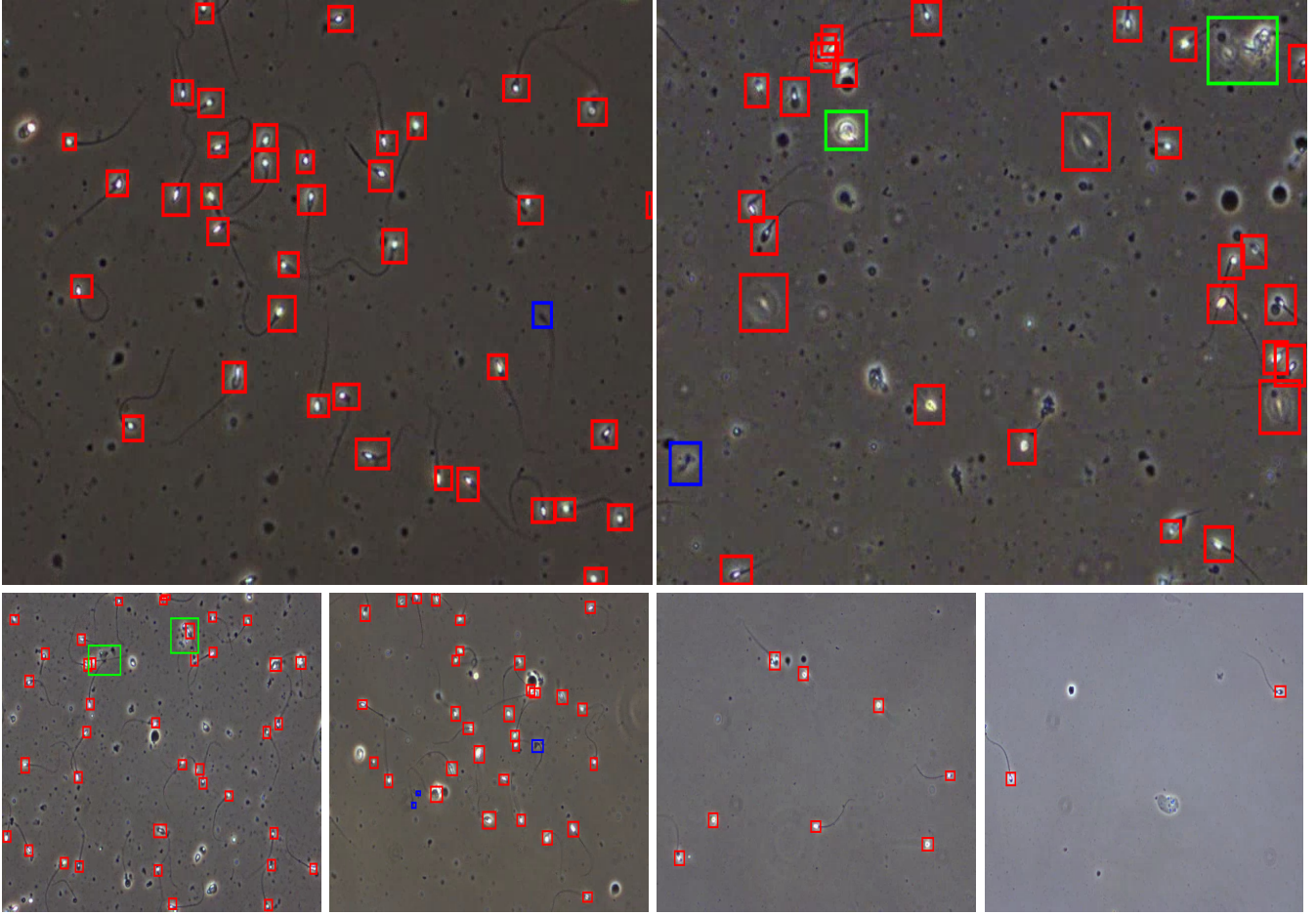


**Figure 1.** Video frames of wet semen preparations with corresponding bounding boxes. Top: large images showing different classes of bounding boxes, red - sperm, green - sperm cluster, and blue - small or pinhead sperm. Bottom: presenting different sperm concentration levels from high to low (from left to right, respectively).

Description	# Count
#annotated 30s video clips	20
Frames per second (FPS) per video	45 – 50
# of annotated frames	29,196
# Frames with at least one sperm	28,974
# Frames with at least one cluster	10,199
# Frames with at least one small or pinhead sperm	13,532
# bounding boxes	656,334
# classes	3 (sperm-0, cluster-1, small or pinhead-2)
# unique sperms (with tracking IDs)	1,121
# unique clusters (with tracking IDs)	20
# unique small or pinheads (with tracking IDs)	35
# unlabeled 30s video clips	336
# remaining 30s video clips from the 20 annotated videos	166

**Table 2.** Summary of quantitative information about VISEM-Tracking dataset.

(videos *video\_35* and *video\_52* have 1,440 total frames, and video *video\_82* has 1,500 total frames). The distribution of the bounding boxes is reflected in Figure 4 - (a), and the 2D histogram on the height and width of the bounding boxes is shown in Figure 4 - (b). Figure 4 - (a) shows that the bounding boxes tend to be evenly distributed across the video frames, with a higher

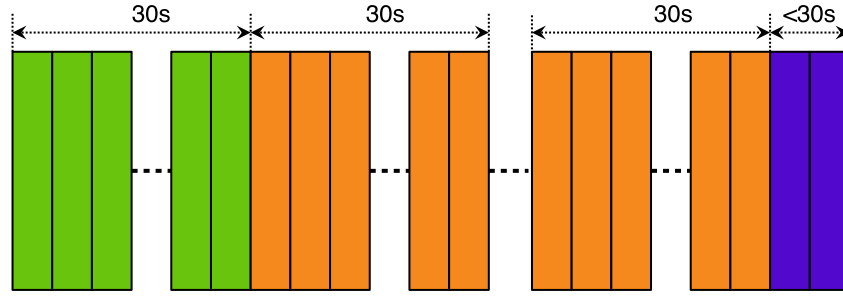


**Figure 2.** Splitting videos into 30 seconds clips. **Green** color represents the split used to manually annotate sperms using bounding boxes. **Orange** color represents the rest of 30s splits included in unlabeled dataset. **Purple** color section represents the last part of a video which does not have 30s long clip. Therefore, we do not include these endings in our dataset to maintain the consistency of 30s clips.

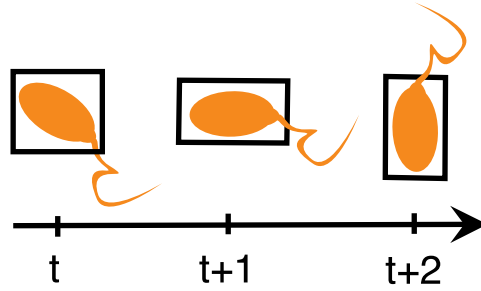


**Figure 3.** Changing bounding box area over time for the same sperm head .

concentration of bounding boxes in the upper left of the video frames. According to Figure 4 - (b), the variation of bounding box size is quite small.

## Technical Validation

We divided the 20 videos into a training data of 16 videos and a validation dataset of 4 videos (video IDs of the validation dataset are provided in the GitHub repository). The training set was used to train **deep learning (DL)** models, and the validation dataset was used to evaluate our baseline **DL** models. YOLOv5<sup>20</sup> was selected as the baseline sperm detection **DNN** model. This version of YOLO consists of five different models, namely, YOLOv5n (nano), YOLOv5s (small), YOLOv5m (medium), YOLOv5l (large), and YOLOv5x (XLarge). All models were trained using the training dataset with a number of class parameters of 3, which include *normal sperm*, *cluster*, and *small or pinhead* categories.

In the training process, we provided extracted frames and the corresponding bounding box details to the YOLOv5 models. We set the image size parameter to 640, batch size to 16, and the number of epochs to 300. All other hyperparameters, such as learning rate, batch size, and optimizer were kept with default values of YOLOv5<sup>2</sup>. Furthermore, all experiments were performed on two NVIDIA GeForce RTX 3080 graphic processing units with a total of 20GB memory (10GB per each GPU) with AMD Ryzen 9 3950X 16-Core Processor. The best model was found using the performance on the validation dataset.

Precision, recall,  $mAP_{0.5}$ ,  $mAP_{0.5 : 0.95}$ , and *fitness value*, as calculated in <sup>20</sup>, were used to measure the performance of different YOLOv5 models. The results are listed in Table 3, showing that YOLOv5l performs best. The fitness value presented in the table is calculated using the following equation, which is used in the YOLOv5 implementation to compare model performance.

$$Fitness\_value = (0.1 \times mAP_{0.5} + 0.9 \times mAP_{0.95})$$

Samples for visual comparisons of predictions from the five models are shown in Figure 5. These predictions are from the first frame of the selected four validation videos.

<sup>20</sup><https://github.com/ultralytics/yolov5>



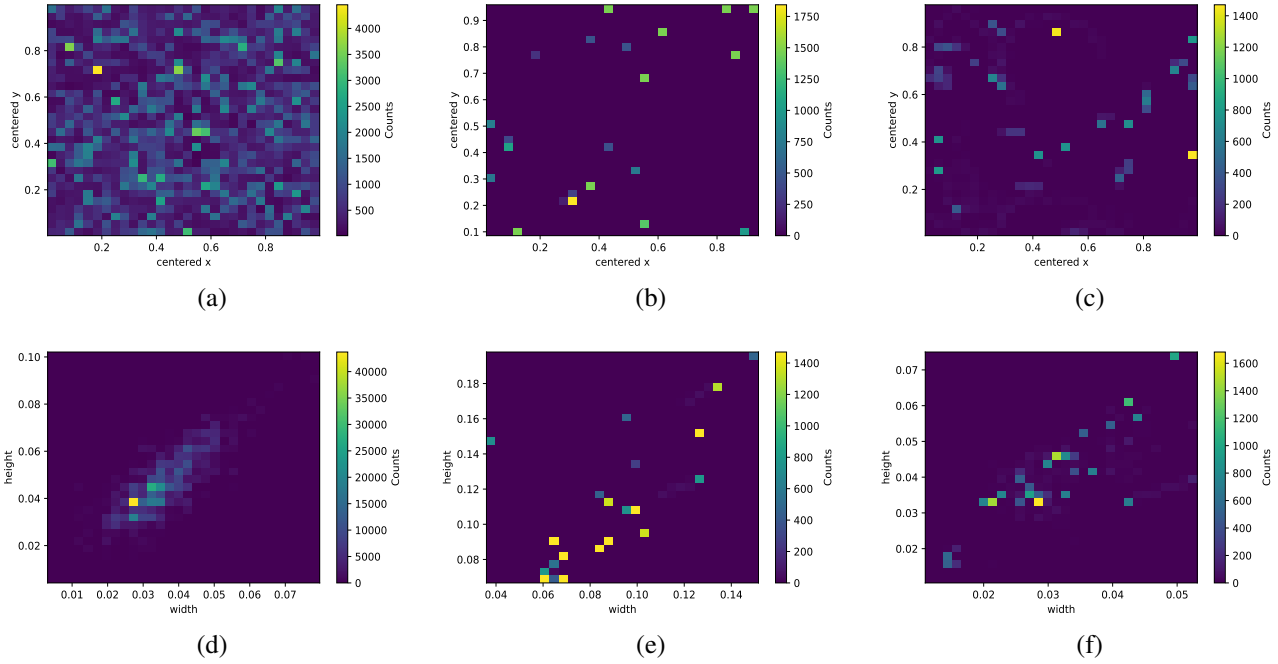


**Figure 4.** Statistics about bounding box coordinates and area. (a) - 2D histogram on the centered coordinates of the bounding boxes of the sperm class. (b) - 2D histogram on the centered coordinates of the bounding boxes of the cluster class. (c) - 2D histogram on the centered coordinates of the bounding boxes of the small and pinhead class. (d) - 2D histogram on the height and width (normalized values) of the bounding boxes of sperm class. (e) - 2D histogram on the height and width (normalized values) of the bounding boxes of the cluster class. (f) - 2D histogram on the height and width (normalized values) of the bounding boxes of the small or pinhead class.

**Table 3.** Different evaluation metrics and corresponding values with the five different YOLOv5 models.

YOLO model	Precision	Recall	mAP_0.5	mAP_0.5:0.95	Fitness value
YOLOv5n	0.4120	0.2380	0.2046	0.0567	0.0715
YOLOv5s	0.4292	0.2560	0.2102	0.0703	0.0843
YOLOv5m	0.5712	0.2279	0.2216	0.0655	0.0811
YOLOv5l	0.4323	0.2550	0.2231	0.0775	0.0920
YOLOv5x	0.3093	0.2517	0.1995	0.0630	0.0766

## Usage Notes

To the best of our knowledge, this is the first dataset containing long human spermatozoa video clips (30 seconds with 45-50 FPS) that are manually annotated with bounding boxes for each spermatozoon. The performance of our DL experiments for detecting spermatozoa shows that the training data provided in this dataset is diverse and can be used to train advanced DL models.

The data enables different future research directions. For example, it can be used to prepare more labeled data using strategies like semi-supervised learning. Researchers can use the labeled data to train a DL model (such as YOLOv5) and predict bounding boxes for the unlabeled data. Then, those pseudo-labeled data can be passed to the experts in the domain to verify them. This method can make the data annotation process easier and produce accurate labeled datasets faster than manual annotations.

Sperm tracking is necessary to determine sperm dynamics and motility levels. We provide tracking IDs to identify the same spermatozoa throughout the video. Using this data, one can train sperm tracking algorithms, and the results of the tracking algorithms can help to identify different biomedical relevant parameters such as velocity and kinematics. Additionally, it is difficult to determine which spermatozoa in a semen sample have the highest motility, which is of clinical importance. The dataset can be used to train such algorithms for finding spermatozoa with the highest motility.

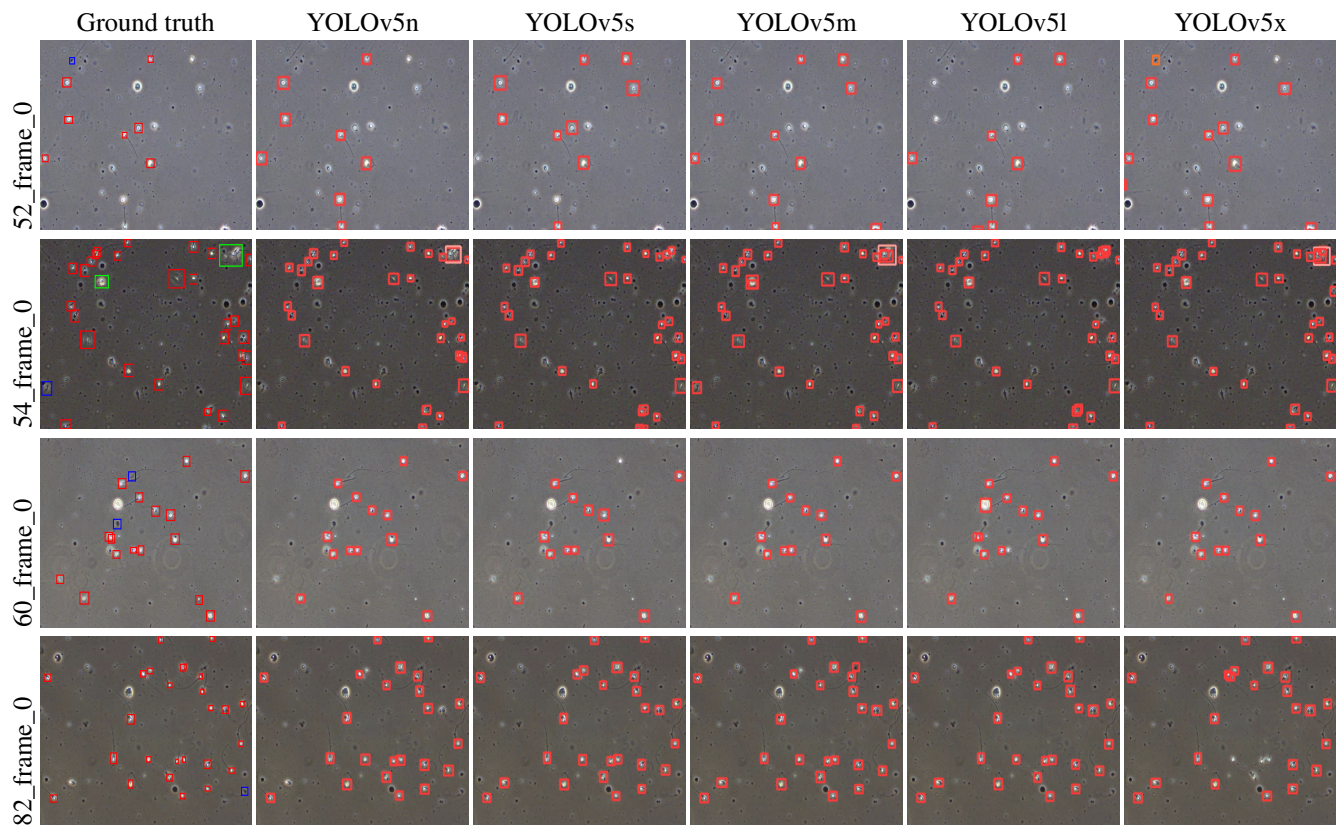


**Figure 5.** Predicted bounding boxes from the different models of YOLOv5 for the first frames of the validation data. Video IDs 82, 60, 54 and 52 were used as validation videos.

In addition to the sperm tracking annotations, we also provide additional metadata for the sperm samples. Using this data, researchers can train models that combine the metadata with the tracking information to obtain more accurate predictions of, for example, motility levels.

There is also a growing interest in exploring synthetic data to address data deficiencies and timely and costly data annotation problems in the medical domain<sup>21</sup>. Researchers can use the dataset to train deep generative models<sup>22,23</sup> to generate synthetic data which then can be used to train other ML models and achieve better generalizable performance. Furthermore, one can train conditional deep generative models<sup>24,25</sup> to generate synthetic sperm data with the corresponding ground truth (bounding boxes) using our dataset to overcome the costly problem of getting annotated data.

Another hot topic in AI and medicine is simulating biological organs or creating digital twins. The dataset can for example be used to extract features of sperm motility to simulate spermatozoa and their behaviors. Simulations of spermatozoa can potentially lead to more accurate models than current solutions in the field.

## Code availability

The full dataset is available at <https://zenodo.org/record/7293726>. The license for the data is Creative Commons Attribution 4.0 International (CC BY 4.0). The code repository with the scripts of data preparations and technical validations (models and pre-trained checkpoints) is available at <https://github.com/simulamet-host/visem-tracking>.

## References

1. Gill, M. E. & Quaas, A. M. Looking with new eyes: advanced microscopy and artificial intelligence in reproductive medicine. *J. Assist. Reproduction Genet.* 1–5 (2022).
2. Riegler, M. A. *et al.* Artificial intelligence in the fertility clinic: status, pitfalls and possibilities. *Hum. Reproduction* **36**, 2429–2442 (2021).

3. Thambawita, V., Halvorsen, P., Hammer, H., Riegler, M. & Haugen, T. B. Stacked dense optical flows and dropout layers to predict sperm motility and morphology. *Proc. MediaEval 2019 CEUR Work.* (2019).
4. Hicks, S. A. *et al.* Machine learning-based analysis of sperm videos and participant data for male fertility prediction. *Sci. reports* **9**, 1–10 (2019).
5. Thambawita, V., Halvorsen, P., Hammer, H., Riegler, M. & Haugen, T. B. Extracting temporal features into a spatial domain using autoencoders for sperm video analysis. *Proc. MediaEval 2019 CEUR Work.* (2019).
6. Javadi, S. & Mirroshandel, S. A. A novel deep learning method for automatic assessment of human sperm images. *Comput. biology medicine* **109**, 182–194 (2019).
7. You, J. B. *et al.* Machine learning for sperm selection. *Nat. Rev. Urol.* **18**, 387–403 (2021).
8. Ghasemian, F., Mirroshandel, S. A., Monji-Azad, S., Azarnia, M. & Zahiri, Z. An efficient method for automatic morphological abnormality detection from human sperm images. *Comput. Methods Programs Biomed.* **122**, 409–420, <https://doi.org/10.1016/j.cmpb.2015.08.013> (2015).
9. Soroush, J. & Seyed, A. M. A novel deep learning method for automatic assessment of human sperm images. *Comput. Biol. Medicine* **109**, 182–194, [10.1016/j.compbiomed.2019.04.030](https://doi.org/10.1016/j.compbiomed.2019.04.030) (2019).
10. Shaker, F., Monadjemi, S. A., Alirezaie, J. & Naghsh-Nilchi, A. R. A dictionary learning approach for human sperm heads classification. *Comput. Biol. Medicine* **91**, 181–190, [10.1016/j.compbiomed.2017.10.009](https://doi.org/10.1016/j.compbiomed.2017.10.009) (2017).
11. Chang, V., Garcia, A., Hitschfeld, N. & Härtel, S. Gold-standard for computer-assisted morphological sperm analysis. *Comput. biology medicine* **83**, 143–150 (2017).
12. Ilhan, H. O., Sigirci, I. O., Serbes, G. & Aydin, N. A fully automated hybrid human sperm detection and classification system based on mobile-net and the performance comparison with conventional methods. *Med. & Biol. Eng. & Comput.* **58**, 1047–1068, [10.1007/s11517-019-02101-y](https://doi.org/10.1007/s11517-019-02101-y) (2020).
13. McCallum, C. *et al.* Deep learning-based selection of human sperm with high DNA integrity. *Commun. biology* **2**, 250, [10.1038/s42003-019-0491-6](https://doi.org/10.1038/s42003-019-0491-6) (2019).
14. Chen, A. *et al.* Svia dataset: A new dataset of microscopic videos and images for computer-aided sperm analysis. *Biocybern. Biomed. Eng.* **42**, 204–214, [10.1016/j.bbe.2021.12.010](https://doi.org/10.1016/j.bbe.2021.12.010) (2022).
15. Haugen, T. B. *et al.* Visem: A multimodal video dataset of human spermatozoa. In *Proceedings of the 10th ACM Multimedia Systems Conference, MMSys '19*, 261–266, [10.1145/3304109.3325814](https://doi.org/10.1145/3304109.3325814) (Association for Computing Machinery, New York, NY, USA, 2019).
16. Organization, W. H. *et al.* Who laboratory manual for the examination and processing of human semen (2010).
17. Andersen, J. M. *et al.* Fatty acid composition of spermatozoa is associated with bmi and with semen quality. *Andrology* **4**, 857–865, <https://doi.org/10.1111/andr.12227> (2016). <https://onlinelibrary.wiley.com/doi/pdf/10.1111/andr.12227>.
18. Boivin, J., Bunting, L., Collins, J. A. & Nygren, K. G. International estimates of infertility prevalence and treatment-seeking: potential need and demand for infertility medical care. *Hum. reproduction* **22**, 1506–1512 (2007).
19. Van Engelen, J. E. & Hoos, H. H. A survey on semi-supervised learning. *Mach. Learn.* **109**, 373–440 (2020).
20. Jocher, G. *et al.* ultralytics/yolov5: v6.2 - YOLOv5 Classification Models, Apple M1, Reproducibility, ClearML and Deci.ai integrations, [10.5281/zenodo.7002879](https://doi.org/10.5281/zenodo.7002879) (2022).
21. Thambawita, V. *et al.* Deepsynthbody: the beginning of the end for data deficiency in medicine. In *2021 International Conference on Applied Artificial Intelligence (ICAPAI)*, 1–8 (IEEE, 2021).
22. Ho, J., Jain, A. & Abbeel, P. Denoising diffusion probabilistic models. *Adv. Neural Inf. Process. Syst.* **33**, 6840–6851 (2020).
23. Goodfellow, I. *et al.* Generative adversarial networks. *Commun. ACM* **63**, 139–144 (2020).
24. Mirza, M. & Osindero, S. Conditional generative adversarial nets. *arXiv preprint arXiv:1411.1784* (2014).
25. Sinha, A., Song, J., Meng, C. & Ermon, S. D2c: Diffusion-decoding models for few-shot conditional generation. *Adv. Neural Inf. Process. Syst.* **34**, 12533–12548 (2021).

## Acknowledgements

The research presented in this paper has benefited from the Experimental Infrastructure for Exploration of Exascale Computing (eX3), which is financially supported by the Research Council of Norway under contract 270053.



## **Author contributions statement**

VT, SAH, and MAR made the conception and design of the work. VT, SAH, AS, HLH, and MAR prepared and annotated data. JA, OW, and TBH reviewed and verified data annotations. VT conceived and conducted the deep learning experiment(s). VT, SAH, AS, TN, and MAR analysed the data and results. VT, AS, SAH, TH, PH, and MAR prepared the draft of the work. All authors reviewed and revised the manuscript.

## **Competing interests**

None of the authors has any competing interests.